Proceedings of the
47th IEEE Conference on Decision and Control
Cancun, Mexico, Dec. 9-11, 2008

Design and performance of *in vitro* transcription rate regulatory circuits

Elisa Franco and Richard M. Murray

Abstract— **This paper proposes a synthetic *in vitro* circuit that aims at regulating the rate of RNA transcription through positive feedback interactions. This design is dual to a previously synthesized transcriptional rate regulator based on self-repression. Two DNA templates are designed to interact through their transcripts, creating cross activating feedback loops that will equate their transcription rates at steady state. A mathematical model is developed for this circuit, consisting of a set of ODEs derived from the mass action laws and Michaelis–Menten kinetics involving all the present chemical species. This circuit is then compared to its regulatory counterpart based on negative feedback. A global sensitivity analysis reveals the fundamental features of the two designs by evaluating their equilibrium response to changes in the most crucial parameters of the system.**

I. Introduction and Background

Building biological machinery out of known components with the same confidence as one can build a silicon chip is one of the crucial objectives of scientists who approach synthetic biology with a quantitative mind. This will not only allow to expand the pool of available molecular architectures but also help to gain a better understanding of the characteristics, modularity and evolvability of existing complex biological networks still to be unraveled [1]. It is fundamental to focus on basic functional motifs that are widely diffused in nature, as they can be considered elementary building blocks of large scale systems [2].

Building a circuit out of biological components is simplified when operating *in vitro*: a higher control over the environment and over unwanted reactions permits to monitor more precisely the functional response of the designed system. Utilizing few components is also beneficial to the same purposes.

Recognizing the extraordinary importance of understanding basic network motifs in a controllable environment, the topic of this paper is the design and modeling of an *in vitro* circuit that aims at regulating the transcription rate of RNA through a positive feedback interconnection. This work follows a previously proposed negative feedback-based circuit having the same objective [4]. Transcription is a fundamental part of the central dogma of molecular biology and is naturally regulated in the cell: for instance it can be turned on or off by binding of transcription factors, or by secondary structure formation in the nascent RNA (see [5] and references cited therein). The dynamics of several genes can be coupled, and it is an interesting question whether there exist mechanisms that match the transcription rates of two or more genes.

The circuit described in this paper is composed of two double stranded DNA (dsDNA) species coupled through their transcripts with a mechanism of cross activation: if one of the two transcripts is in stoichiometric excess, it is designed to increase the production of the other RNA species by releasing a single stranded DNA (ssDNA) activator molecule. Thanks to this positive feedback loop, at equilibrium the two transcription rates are equal. This feature is attractive because it is a first step towards the design of concentration-following circuits. The objective of our future work is in fact to understand how positive and negative feedback motifs can be used in order to keep a molecular species of interest at a desired concentration level, or make it track a certain concentration time profile.

The first *in vitro* transcriptional switches were designed and synthesized by Kim [9], [8] as a possible biological implementation of neural networks. More complex cell–free environments for quantitative analysis have been proposed in [11], where protein signaling patterns are considered. However, the computational power of a simple setting comprising only nucleic acids and few enzymes has been theoretically proven to be superior [7] by virtue of its simplicity. The same thermodynamics principles utilized to build transcriptional switches are useful to construct several other systems presenting a circuit–like behavior [12], [15] or even to create nanomolecular devices [3], [13]. A further motivation in focusing our attention on nucleic acids lies in their important role in the control of gene expression, which is being acknowledged and studied with increasing interest [5].

This paper, building on previous work that analyzed a negative feedback rate regulator [4], proposes its positive feedback counterpart. The performance and features of the two different designs are compared through a global sensitivity analysis with respect to their feedback interconnection and the environment enzymatic levels. These two architectures based on transcriptional switches create a regulatory mechanism not considered before. Following the procedure in [4], the positive feedback rate regulator was designed and mathematically modeled starting from the occurring biochemical reactions; this new system is currently being synthesized in laboratory. The employed pool of biological machinery is of interest because it can be used to construct a variety of molecular devices with different functionalities, despite its simplicity and low number of components.

Research supported in part by the Institute for Collaborative Biotechnologies through grant DAAD19-03-D-0004 from the U.S. Army Research Office.

The authors are with the Division of Engineering and Applied Sciences, California Institute of Technology, Pasadena, CA 91125. elisa,murray@cds.caltech.edu.

II. Circuit description and modeling

A. Circuit design

The first objective of this work is that of proposing a new synthetic transcription rate regulatory network relying on positive feedback, as an alternative to the negative feedback based circuit described in [4]. The two design ideas are schematically compared in Figure 1a and 1b.

Transcriptional circuits are composed of nucleic acids and few enzyme species [9], [8]. The core of these circuits are DNA templates (100–120 nucleotides long) designed to be transcribed into RNA (80–100 nucleotides long) in the presence of the enzyme RNA polymerase ($\mathbf{R_p}$). This process can be switched on or off by displacement of part of the enzyme binding area (the promoter). The ssDNA sequences allowing completion of the promoter are called activators (25–35 nucleotides long), which can be sequestered by ssDNA (or RNA) sequences called inhibitors (25-35 nucleotides long).

In the positive feedback rate regulator, two templates T_1, T_2 are incomplete in their promoter region: activators A_1, A_2 can bind the templates completing the promoter and allowing $\mathbf{R_p}$ to operate the transcription of RNA species R_1, R_2. Transcription is normally off due to the presence of two ssDNA inhibitor strands S_1, S_2, that sequester the activators. When transcription is initiated, the two RNAs are designed to bind to each other, forming a double stranded complex potentially available for further processing. By construction, either product in excess with respect to the other will promote the production of the other species by binding to its inhibitor, thereby releasing the corresponding activator. Since both transcripts have this cross-activation feature, at steady state their production rates should be equal, as demonstrated in Section III. RNase H ($\mathbf{R_h}$), the other enzyme species present, allows degradation of DNA-RNA hybrids, introducing a further level of dynamic adaptation. This architecture is schematically described in Figure 1 a).

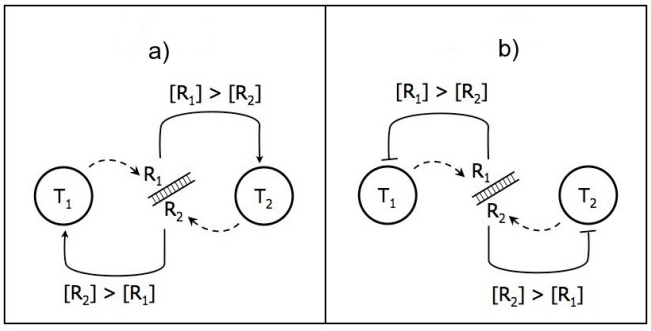

Fig. 1. Schematic representation of a) positive and b) negative feedback rate regulators

The mechanism that allows turning on and off the templates is known as branch migration. Nucleic acid strands provided with *toehold* regions [14] that remain exposed in bound states can be displaced by specifically designed RNA or DNA molecules. In our case, the RNA transcripts 'encode' for the inhibitor toehold and can initiate the strand displacement. For instance, we can design A_1 so that it binds to S_1 with free energy of -35 kcal/mol, and R_1 so that it binds to S_1 with free energy of -40 kcal/mol: the second will thus be a more favorable reaction.

The strand design method consists of finding the desired complementarity regions and energetic constraints. This procedure can be automated by using Monte-Carlo optimization of a user defined scoring function where the free energy gain of unwanted secondary structures is suitably weighted (in house software of the E. Winfree Lab at Caltech). Our design for the strands is shown in Figure 2: following the idea proposed in [4], the RNA transcripts will have 'mirrored' sequences in order to satisfy complementarity and cross activation. As in the negative feedback rate regulatory circuit, this design can produce unwanted interactions among the strands. Specifically there will be a further off state of the templates due to the binding of R_i to T_j. Moreover, given that each RNA species also encodes for its activator complementary sequence, there could be a self-inhibitory action for each subsystem: this effect can be limited to R_i binding to free A_i if the activator toehold region is not present in the RNA sequence (therefore R_i will not be able to strip off A_i from the template T_i). The system behavior can be monitored by labeling the DNA strands with fluorescent dyes and quenchers [10], as detailed in Figure 2.

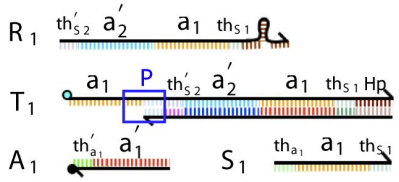

Fig. 2. Design for the positive feedback regulator, sub–circuit of index 1. The arrow tick at the end of the strands indicates the $5^{'}$ to $3^{'}$ direction. Starting from the $5^{'}$ (left): fluorophore (cyan circle); a_1 region (orange) including part of the promoter region (blue box); initiation sequences (cyan); complementary toehold th_{S_2} region (light purple); complementary $a_2^{'}$ region (light blue); a_1 region (orange); toehold th_{S_2} region (light green) and at the $3^{'}$ end *hairpin* region (brown). The hairpin is necessary to avoid spurious elongation of the RNA strand during transcription [8]. The sequence of the transcript R_1 comprises all the regions of T_1 right after the promoter. Starting from the 3' end (left) for A_1: quencher (black circle); toehold th_{a_1} region (green); activator $a_1^{'}$ region (red) comprising part of the promoter.

B. Mathematical modeling

The chemical reactions occurring in the system are used to derive a set of ordinary differential equations (ODEs). Throughout this derivation, the dissociation constants are omitted when assumed to be negligible. For enzymatic reactions, we assume that the concentration of enzymes is considerably lower than that of the DNA molecules, allowing the classical steady state assumption for Michaelis-Menten kinetics. The use of a deterministic continuous model is well justified in this context: the experimental setting of transcriptional circuits is such that the molecular concentrations are in the order of 10^9 units per microliter. This case is dramatically different from, for instance, certain transcription factors in cellular environments, which could be 9 orders of magnitude less concentrated; stochastic modeling is necessary in those cases.

The mass action reactions are, for $i \in \{1,2\}$, $j \in \{2,1\}$:

$$\begin{aligned}
&\text{Activation} && T_i + A_i \overset{k_{T_iA_i}}{\rightarrow} T_iA_i \\
&\text{Inhibition} && T_iA_i + S_i \overset{k_{T_iA_iS_i}}{\rightarrow} T_i + S_iA_i \\
& && A_i + S_i \overset{k_{A_iS_i}}{\rightarrow} A_iS_i \\
&\text{Release} && R_i + A_jS_j \overset{k_{R_iA_jS_j}}{\rightarrow} R_iS_j + A_i \\
& && R_i + S_j \overset{k_{R_iS_j}}{\rightarrow} R_iS_j \\
&\text{Output formation} && R_i + R_j \overset{k_{R_iR_j}}{\rightarrow} R_iR_j \\
&\text{Unwanted interactions} && R_i + A_i \overset{k_{R_iA_i}}{\rightarrow} R_iA_i \\
& && R_i + T_j \overset{k_{R_iT_j}}{\rightarrow} R_iT_j
\end{aligned} \tag{1}$$

The target enzymatic reactions are:

$$\begin{aligned}
&\mathbf{R_p} + T_iA_i \underset{k^-_{ON_{ii}}}{\overset{k^+_{ON_{ii}}}{\rightleftarrows}} \mathbf{R_p} \cdot T_iA_i \overset{k_{catON_{ii}}}{\rightarrow} \mathbf{R_p} + T_iA_i + R_i \\
&\mathbf{R_p} + T_i \underset{k^-_{OFF_i}}{\overset{k^+_{OFF_i}}{\rightleftarrows}} \mathbf{R_p} \cdot Ti \overset{k_{catOFF_i}}{\rightarrow} \mathbf{R_p} + T_i + R_i \\
&\mathbf{R_h} + R_iS_j \underset{k^-_{H_{S_j}}}{\overset{k^+_{H_{S_j}}}{\rightleftarrows}} \mathbf{R_h} \cdot R_iS_j \overset{k_{catH_{S_j}}}{\rightarrow} \mathbf{R_h} + S_j
\end{aligned} \tag{2}$$

The enzymatic processes involving unwanted complexes:

$$\begin{aligned}
&\mathbf{R_p} + R_iT_j \underset{k^-_{OFF_{ij}}}{\overset{k^+_{OFF_{ij}}}{\rightleftarrows}} \mathbf{R_p} \cdot R_iT_j \overset{k_{catOFF_{ij}}}{\rightarrow} \mathbf{R_p} + R_iT_j + R_j \\
&\mathbf{R_h} + R_iA_i \underset{k^-_{H_{A_i}}}{\overset{k^+_{H_{A_i}}}{\rightleftarrows}} \mathbf{R_h} \cdot R_iA_i \overset{k_{catH_{A_i}}}{\rightarrow} \mathbf{R_h} + A_i \\
&\mathbf{R_h} + R_iT_j \underset{k^-_{H_{T_j}}}{\overset{k^+_{H_{T_j}}}{\rightleftarrows}} \mathbf{R_h} \cdot R_iT_j \overset{k_{catH_{T_j}}}{\rightarrow} \mathbf{R_h} + T_j
\end{aligned} \tag{3}$$

Given equations (1), (2), and (3) it is straightforward to derive a set of ODEs as follows:

$$\begin{aligned}
\frac{d}{dt}[T_i] =& -k_{T_iA_i}[T_i][A_i] - k_{R_jT_i}[R_j][T_i] \\
&+ k_{catH_{T_i}}[Rh \cdot R_jT_i] \\
\frac{d}{dt}[A_i] =& -k_{T_iA_i}[T_i][A_i] - k_{A_iS_i}[A_i][S_i] - k_{R_iA_i}[R_i][A_i] \\
&+ k_{R_jA_iS_i}[R_j][A_iS_i] + k_{catH_{A_i}}[\mathbf{R_h} \cdot R_iA_i] \\
\frac{d}{dt}[S_i] =& -k_{A_iS_i}[A_i][S_i] - k_{T_iA_iS_i}[T_iA_i][S_i] \\
&- k_{R_jS_i}[R_j][S_i] + k_{catH_{S_i}}[\mathbf{R_h} \cdot R_jS_i] \\
\frac{d}{dt}[R_i] =& -k_{R_iA_jS_j}[R_i][A_jS_j] - k_{R_iR_j}[R_i][R_j] \\
&- k_{R_iT_j}[R_i][T_j] - k_{R_iS_j}[R_i][S_j] - k_{R_iA_i}[R_i][A_i] \\
&+ k_{catON_{ii}}[\mathbf{R_p} \cdot T_iA_i] + k_{catOFF_i}[\mathbf{R_p} \cdot T_i] \\
&+ k_{catOFF_{ji}}[\mathbf{R_p} \cdot R_jT_i] \\
\frac{d}{dt}[R_iT_j] =& +k_{R_iT_j}[R_i][T_j] - k_{catH_{T_j}}[\mathbf{R_h} \cdot R_iT_j] \\
\frac{d}{dt}[R_iR_j] =& +k_{R_iR_j}[R_i][R_j]
\end{aligned} \tag{4}$$

Where $[T_i]$ represents the concentration of species T_i. The molecular complexes that appear on the right hand side of the above equation can be expressed as a function of the states with some standard steps. Mass conservation immediately yields the dynamics of $[T_iA_i]$, $[A_iS_i]$, $[R_iS_j]$.

Assuming that binding of the enzyme is faster than transcription or degradation in equations (2) and (3), and defining the Michaelis–Menten coefficients (e.g. for the on state of the template $k_{MONii} = \frac{k_{-ONii}+k_{catONii}}{k_{+ONii}}$), it is possible to use mass conservation laws to obtain explicit expressions for the enzyme concentrations. Due to space limitations we only report the complete expression for the term forR_p bound to $[T_iA_i]$:

$$[\mathbf{R_p}T_iA_i] = \frac{[\mathbf{R_p}^{tot}]}{(1 + \sum_{i,j}\frac{[T_iA_i]}{k_{MON_{ii}}} + \frac{[T_i]}{k_{MOFF_i}} + \frac{[R_iT_j]}{k_{MOFF_{ij}}})} \tag{5}$$

The nonlinear set of equations (4) was numerically analyzed using the MATLAB ode23s solver. The parameter values used in these simulations are reported in Table I. These parameters are taken from the literature [8] and from experimental data fitting on the negative feedback regulator (data not shown here), and they are chosen so that the two sub-circuits are identical. This is a simplifying assumption that helps to provide intuition on the performance of the circuit by just creating an imbalance in the concentration of the strands. In particular, utilizing the parameters listed in Table I, and initial conditions $T_1^{tot} = 100n$M, $A_1^{tot} = 100n$M, $S_1^{tot} = 100n$M, $T_2^{tot} = 200n$M, $A_2^{tot} = 200n$M and $S_2^{tot} = 200n$M. The enzymatic concentrations are $\mathbf{R_p}^{tot} = 20n$M and $\mathbf{R_h}^{tot} = 2n$M. These initial conditions are chosen based on the amounts normally utilized in an experimental setting and are targeted for reaction volumes of 70μL. The dynamics of T_1, T_2 on and of the total amount of RNA produced are shown in Figure 3, simulated over a 6 hour time window.

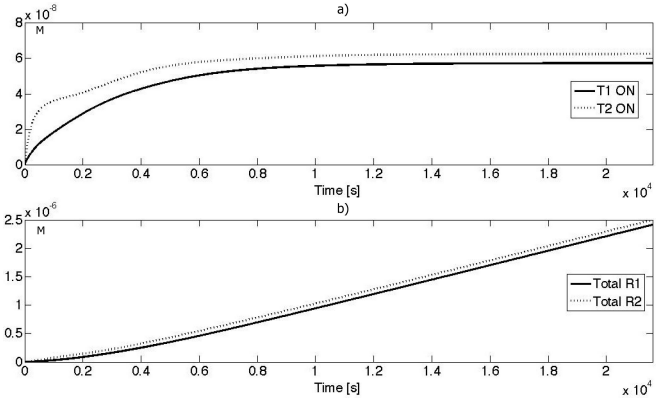

Fig. 3. a) Time profile of the templates in on state. b) Time profile of the total amount of produced RNA transcripts

III. Positive and negative feedback design comparison

A. Rate regulation

The models for the positive and negative feedback rate regulator [4] can be simplified by eliminating negligible dynamics and unwanted interactions. The negligible dynamics

are represented by transcription reactions that may occur when the templates are off (not bound to their activator), or when they are bound to an RNA species. The unwanted interactions are those due to the specific design choice, but may be eliminated with a more sophisticated design. The binding reactions between RNA species and DNA templates fall in this latter category; for the positive feedback-based circuit, the binding between the RNA product and its own activator is also considered an unwanted interaction. These simplifications are be helpful in order to study the fundamental features of the two types of feedback.

Referring to the negative feedback circuit dynamics derived in [4], we can write the following simplified equations, where the off transcription reactions and the binding of R_iT_j have been eliminated:

$$\begin{aligned}
\frac{d}{dt}[T_i] &= -\,k_{T_iA_i}\,[T_i]\,[A_i] + k_{R_iT_iA_i}\,[R_i]\,[T_iA_i] \\
\frac{d}{dt}[A_i] &= -\,k_{T_iA_i}\,[T_i]\,[A_i] + k_{catHii}\,[\mathbf{R_h}\cdot R_iA_i] \\
\frac{d}{dt}[R_i] &= -\,k_{R_iR_j}\,[R_i]\,[R_j] - k_{R_iT_iA_i}\,[R_i]\,[T_iA_i] - \\
&\quad + k_{catONii}\,[\mathbf{R_p}\cdot T_iA_i] \\
\frac{d}{dt}[R_iR_j] &= +\,k_{R_iR_j}\,[R_i]\,[R_j]
\end{aligned} \tag{6}$$

For the positive feedback circuit just introduced, the equations can be simplified as follows, by neglecting the off transcription reactions, the binding of R_iT_j and of R_iA_i:

$$\begin{aligned}
\frac{d}{dt}[T_i] &= -\,k_{T_iA_i}\,[T_i]\,[A_i] + k_{R_iT_iA_i}\,[R_i]\,[T_iA_i] \\
\frac{d}{dt}[A_i] &= -\,k_{T_iA_i}\,[T_i]\,[A_i] - k_{A_iS_i}\,[A_i]\,[S_i] \\
&\quad + k_{R_jA_iS_i}\,[R_j]\,[A_iS_i] \\
\frac{d}{dt}[S_i] &= -\,k_{A_iS_i}\,[A_i]\,[S_i] - k_{T_iA_iS_i}\,[T_iA_i]\,[S_i] \\
&\quad - k_{R_jS_i}\,[R_j]\,[S_i] + k_{catH_{S_i}}\,[\mathbf{R_h}\cdot R_jS_i] \\
\frac{d}{dt}[R_i] &= -\,k_{R_iA_jS_j}\,[R_i]\,[A_jS_j] + k_{catON_{ii}}\,[\mathbf{R_p}\cdot T_iA_i] \\
&\quad - k_{R_iR_j}\,[R_i]\,[R_j] - k_{R_iS_j}\,[R_i]\,[S_j] \\
\frac{d}{dt}[R_iR_j] &= +\,k_{R_iR_j}\,[R_i]\,[R_j].
\end{aligned} \tag{7}$$

It is possible to prove that for both designs the steady state transcription rate of R_1 is equal to that of R_2. For the negative feedback circuit, write $[R_i^{tot}] = [R_i] + [R_iA_i] + [R_iR_j]$. Taking the derivative with respect to time, one can immediately see that $\frac{d}{dt}[R_i] = 0 = \frac{d}{dt}[R_iA_i]$, provided that the concentration of two species reaches an equilibrium. Therefore one is left with $\frac{d}{dt}[R_1^{tot}] = \frac{d}{dt}[R_1R_2] = \frac{d}{dt}[R_2^{tot}]$. Analogously for the positive feedback circuit, where $[R_i^{tot}] = [R_i] + [R_iS_j] + [R_iR_j]$, one shows that when all the other species in the solution have reached a steady state, $\frac{d}{dt}[R_1^{tot}] = \frac{d}{dt}[R_2^{tot}] = \frac{d}{dt}[R_1R_2]$. Note that the notation $[R_i]$ indicates the concentration of the ith RNA species which is not bound to other molecules.

The transient dynamics of $[R_i^{tot}]$ can be evaluated by explicitly writing their expression, where several terms will cancel out. For the negative feedback regulatory circuit one is left with the equation: $\frac{d}{dt}[R_i^{tot}] = k_{catON_{ii}}\,[\mathbf{R_p}\cdot T_iA_i] - k_{catHii}\,[\mathbf{R_h}\cdot R_iA_i]$. For the positive feedback regulator one gets: $\frac{d}{dt}[R_i^{tot}] = k_{catON_{ii}}\,[\mathbf{R_p}\cdot T_iA_i] - k_{catH_{SJ}}\,[\mathbf{R_h}\cdot R_iS_j]$. It is clear from these expressions that, if one assumes identical binding parameters for the two sub-circuits, in order to experimentally verify $\frac{d}{dt}[R_1^{tot}] = \frac{d}{dt}[R_2^{tot}]$ one should be able to measure both concentrations of $[T_iA_i]$ and $[R_iA_i]$ (negative feedback circuit) or $[R_iS_j]$ (positive feedback circuit). While by using fluorescent dyes one can easily estimate $[T_iA_i]$ and use it as an indicator of the transcription rate; measuring $[R_iS_j]$ may not be as straightforward.

B. Sensitivity analysis

The basic architecture of the positive and negative feedback rate regulatory circuits is such that the objective of equating the transcription rates of two sub-circuits will always be fulfilled, when the initial conditions allow the system to reach a steady state (excluding the dsRNA species R_1, R_2 which is not degraded). It is of interest to understand what is the variability of performance due to changes of certain critical parameters of the system.

Local sensitivity analysis restricted to a first order Taylor series approximation was insufficient for this class of nonlinear systems. In fact, the sensitivity matrix technique [6] did not yield meaningful results, due to the large integration times and the type of nonlinearities. The analysis is therefore explored numerically, by tuning the parameters in a certain range and observing the variation in the solution of the ODEs. Attention will be restricted to a limited number of interesting parameters: the feedback strength (self inhibition and cross activation binding rates), the concentration of $\mathbf{R_p}$ and of $\mathbf{R_h}$. The feedback strength can be modulated by changing the length of the toeholds. The enzymatic concentration is often a source of experimental uncertainty, as vendors only provide information about the activity of the protein, defined as moles of substrate converted per unit time.

Figures 4 and 5 show the simulation results for the steady state amount of templates and the transcription rate versus fold change in the parameter of interest. It is meaningful to analyze the steady state behavior of the templates since it is the most directly measurable concentration. The production rate of RNA will also be evaluated, since the objective of the design is that of equating such rate for the two transcripts. The initial conditions were set to $T_1 = 100n$M, $A_1 = 100n$M, $T_2 = 200n$M and $A_2 = 200n$M for the negative feedback circuit. For the positive feedback regulator: $T_1 = 100n$M, $A_1 = 100n$M, $S_1 = 100n$M, $T_2 = 200n$M, $A_2 = 200n$M and $S_2 = 200n$M. The nominal parameters utilized in the simulations are reported in Tables I and II; such parameters have been taken from the literature [8] and from data fits performed on analogous circuits. The nominal concentration of enzymes are $\mathbf{R_p}^{tot} = 20n$M, $\mathbf{R_h}^{tot} = 2n$M, based on experimental practice. This sensitivity analysis was also performed on the full models of the two systems, giving no relevant difference with respect to the reported results (data not shown).

For the negative feedback circuit, Figures 4a and 4b), one can see that both high feedback gain and high $\mathbf{R_p}$

concentration will decrease the equilibrium amount of T_iA_i on. For the positive feedback circuit, Figures 5a and 5b, the effect is instead that of increasing the amount of T_iA_i on. On the other hand, the steady state rate of production of RNA responds in a very different way to a variation of the two parameters. In Figures 4d and 4e one observes that strong self inhibition will obviously decrease the production of RNA for the negative feedback circuit, while a high concentration of $\mathbf{R_p}$ will boost it. As for the positive feedback case, in Figures 5d and 5e show that a strong cross activation will increase up to a certain saturation value the rate of production, while the increment is almost linear with respect to the $\mathbf{R_p}$ amount. Finally, the concentration of $\mathbf{R_h}$ has similar effects on the concentration of templates on and on the rate of production: for the negative feedback circuit, Figures 4c and 4 f, a more significant degradation of RNA-DNA hybrid R_iA_i means more A_i capable of turning the circuit on, and accordingly a higher yield of RNA. On the other hand, the opposite effect is observed in the positive feedback circuit, in Figures 5c and 5f, where degradation of R_iS_j puts back into the circuit the inhibitor S_i.

Given the above analysis, the choice of a particular design will depend on the performance specifications. Clearly the superposition principle does not hold since the systems are nonlinear. The two sub-circuits will reach the same production rate of RNA using both designs: but feasibility constraints should be taken into consideration. For instance, operating at high feedback strength is better, since long toeholds would make the branch migration process faster [14]. Working with low amount of enzymes is also an advantage, as they represent the most costly component of the circuits. The negative feedback rate regulatory circuit has a clear advantage over the positive feedback one in its lower number of DNA species, which make it a simpler and cheaper circuit.

As an example, suppose an overall low amount of RNA is desired. The negative feedback circuit should be utilized, operating at 'high feedback gain' and low $\mathbf{R_p}$, as shown in Figures 6a and 6b (self inhibition binding rates ten times higher than nominal, $\mathbf{R_p} = 10n$). A low amount of RNA could be obtained also using the positive feedback regulatory circuit, at the expense of either using more $\mathbf{R_h}$ or designing short toeholds for the cross–activation process, which would make the reactions slower. If instead the objective is a higher production of RNA, positive feedback loops should be used, with a high cross activation interconnection and low concentration of $\mathbf{R_h}$, Figures 6c and 6d (cross activation ten times higher, $\mathbf{R_h} = 1nM$). A high amount of RNA could be obtained also with the negative feedback loops, utilizing though more $\mathbf{R_p}$ and short toeholds (more expensive and slower reactions).

IV. Conclusions and Future Work

A circuit aimed at matching the transcription rate of two DNA templates has been presented in this paper. The circuit design is based on positive feedback and is an alternative to a previously described circuit based on negative feedback [4].

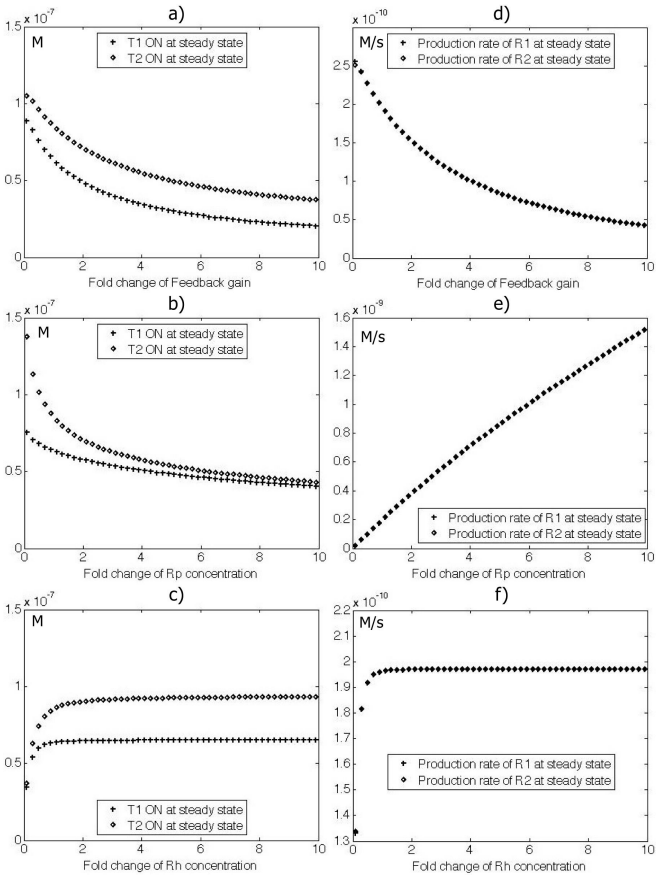

Fig. 4. Steady state sensitivity analysis of the negative feedback rate regulator: a), b) and c) show the equilibrium concentrations of T_1A_1 and T_2A_2 versus the fold change of self inhibition binding rates, $\mathbf{R_p}$ and $\mathbf{R_h}$ amounts; d), e) and f) show the corresponding production rate of RNA under the same conditions. The simulation time is of 6 hours.

TABLE I

Positive feedback regulatory circuit parameters

Units: $[s/M]$	Units: $[1/s]$	Units: $[M]$
$k_{T_iA_i} = 4 \cdot 10^3$	$k_{catON_{ii}} = 0.064$	$k_{MON_{ii}} = 250 \cdot 10^{-9}$
$k_{T_iA_iS_i} = 4 \cdot 10^4$	$k_{catOFF_i} = 1 \cdot 10^{-3}$	$k_{MOFF_i} = 1 \cdot 10^{-6}$
$k_{A_iS_i} = 5 \cdot 10^4$	$k_{catOFF_{ij}} = 1 \cdot 10^{-3}$	$k_{MOFF_{ij}} = 1 \cdot 10^{-6}$
$k_{R_iA_iS_i} = 9 \cdot 10^4$	$k_{catH_{S_i}} = .106$	$k_{MH_{S_i}} = 50 \cdot 10^{-9}$
$k_{R_iS_i} = 9 \cdot 10^4$	$k_{catH_{T_i}} = .106$	$k_{MH_{T_i}} = 50 \cdot 10^{-9}$
$k_{R_iT_j} = 1 \cdot 10^3$		
$k_{R_iA_i} = 1 \cdot 10^3$		
$k_{R_iR_j} = 2 \cdot 10^5$		

TABLE II

Negative feedback regulatory circuit parameters

Units: $[s/M]$	Units: $[1/s]$	Units: $[M]$
$k_{T_iA_i} = 4 \cdot 10^3$	$k_{catON_{ii}} = 0.064$	$k_{MON_{ii}} = 250 \cdot 10^{-9}$
$k_{T_iA_iR_i} = 5 \cdot 10^4$	$k_{catH_{ii}} = .106$	$k_{MH_{ii}} = 50 \cdot 10^{-9}$
$k_{A_iR_i} = 5 \cdot 10^4$		
$k_{R_iR_j} = 2 \cdot 10^5$		

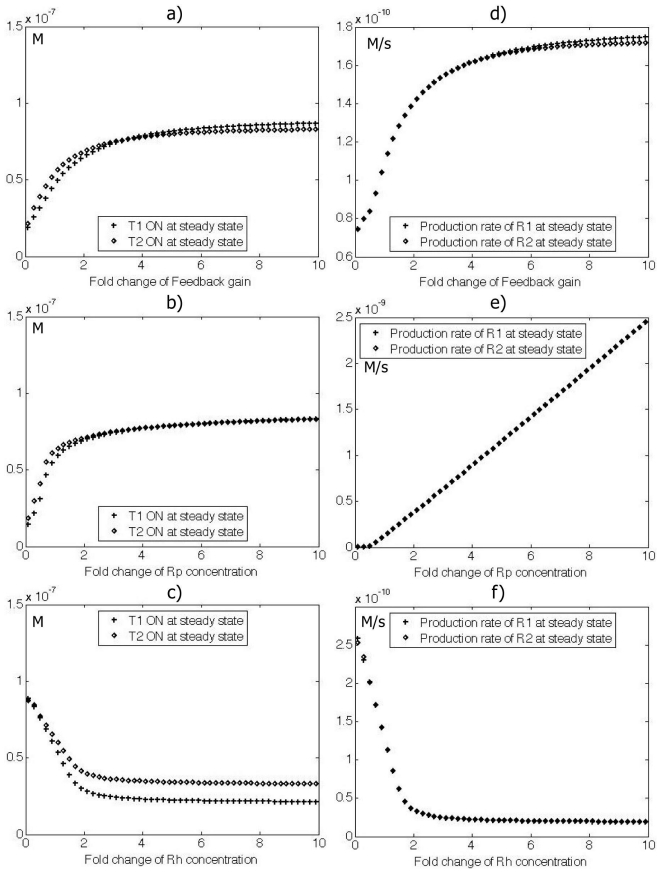

Fig. 5. Steady state sensitivity analysis of the positive feedback rate regulator: a), b) and c) show the equilibrium concentrations of T_1A_1 and T_2A_2 versus the fold change of cross activation binding rates, $\mathbf{R_p}$ and $\mathbf{R_h}$ amounts; d), e) and f) show the corresponding production rate of RNA under the same conditions. The simulation time is of 6 hours.

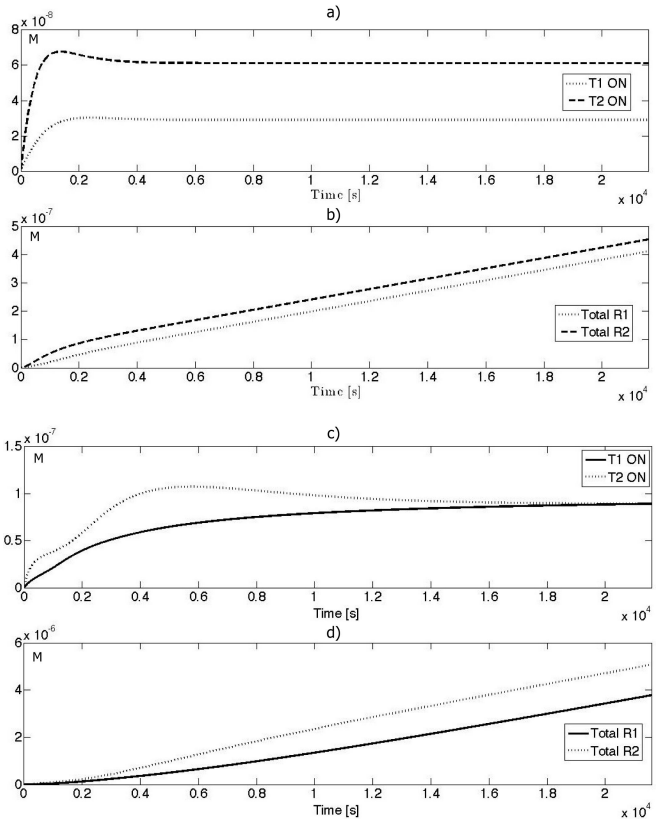

Fig. 6. Design choices to achieve different performances: a) and b) show the time profile of templates on and total production of RNA for the negative feedback circuit with high self inhibition and low amount of $\mathbf{R_p}$; c) and d) show the positive feedback circuit performance with high cross activation and low amount of $\mathbf{R_h}$. The production of RNA in b) is one order of magnitude higher than in d).

A mathematical model of the positive feedback-based regulatory circuit has been derived along with the basic design idea, showing that the theoretical properties of the circuit are as anticipated by physical intuition. A sensitivity analysis has been carried out, comparing the performance of both versions of the rate regulatory architecture. Undergoing work is aimed at experimentally verifying the two circuit properties and the tradeoffs between positive and negative regulation. Future work will focus on how to design concentration followers with transcriptional circuits, starting from the rate regulatory systems. The objective is that of understanding how to match the concentration of two molecules with accuracy through a specific feedback motif. This will allow us to gain more insight on how living organisms perform this feature, maintaining precise concentration levels of their molecular components.

Acknowledgments The authors would like to thank Erik Winfree, Jongmin Kim, Per-Ola Forsberg and all the members of the DNA and Natural Algorithms group at Caltech for their helpful advise during the development of this project.

REFERENCES

[1] Alon, U. An Introduction to Systems Biology: Design Principles of Biological Circuits. Chapman & Hall/CRC, 2006

[2] Alon, U. Network Motifs: Theory and Experimental Approaches. Nature Reviews Genetics, 2007, 8, 450-461

[3] Bishop, J. and Klavins, E. An Improved Autonomous DNA Nanomotor. Nano Letters, 2007, 9, 2574-7

[4] Franco, E., Forsberg, P.-O. and Murray, R. M. Design, modeling and synthesis of an *in vitro* transcription rate regulatory circuit. Proc. of the American Control Conference, June 2007, Seattle, WA. To appear. Available online: http://www.cds.caltech.edu/∼elisa/Publications_files/FFM_ACC08.pdf.

[5] Isaacs, F. J., Dwyer, D. J. and Collins, J. J. RNA synthetic biology. Nature Biotechnology, 2006, 24, 545-554

[6] Khalil, H. K. Nonlinear Systems. Pearson Higher Education, 2002

[7] Kim, J., Hopfield J. J. and Winfree, E. Neural Network Computation by in vitro Transcriptional Circuits. Advances in Neural Information Processing Systems (NIPS), 2004, 17, 681-688

[8] Kim, J., White, K. S. and Winfree, E. Construction of an In Vitro Bistable Circuit from Synthetic Transcriptional Switches. Molecular Systems Biology, 2006, 2:68

[9] Kim, J. In Vitro Synthetic Transcriptional Networks. California Institute of Technology, 2006

[10] Marras, S. A. E. and Kramer, F. R. and Tyagi, S. Efficiencies of fluorescence resonance energy transfer and contact-mediated quenching in oligonucleotide probes. Nucl. Acids Res., 30, 2002

[11] Noireaux, V., Bar-Ziv, R. and Libchaber, A. Principles of cell-free genetic circuit assembly. Proc. Of The National Academy Of Sciences Of The United States Of America, 2003, 100, 12672-12677

[12] Seelig, G., Soloveichik, D., Zhang, D. Y. and Winfree, E. Enzyme-free nucleic acid logic circuits. Science, 2006, 314, 1585-1588

[13] Yin, P., Choi, H. M. T., Calvert, C. R., and Pierce, N. A. Programming Biomolecular Self-Assembly Pathways. Nature, 2008, 451:318-322

[14] Yurke, B. and Mills, A. P. Using DNA to Power Nanostructures. Genetic Programming and Evolvable Machines, 2003, 4, 111-122

[15] Zhang, D. Y., Turberfield, A. J., Yurke, B., and Winfree, E. Engineering Entropy-Driven Reactions and Networks Catalyzed by DNA Science, 2007, 318 (5853), 1121.